- A Comparison Of
Lunar Landing Trajectory Strategies
Using Numerical Simulations -

/ Mike Loucks
/ John Carrico
/ Timothy Carrico
/ Chuck Deiterich

A COMPARISON OF LUNAR LANDING TRAJECTORY STRATEGIES USING NUMERICAL SIMULATIONS

Mike Loucks[1], John Carrico[2], Timothy Carrico[2], Chuck Deiterich[3]

[1]Space Exploration Engineering Co.687 Chinook Way, Friday Harbor WA 98250 360-378-7168 loucks@see.com
[2]Analytical Graphics Inc. 220 Valley Creek Blvd. Exton, PA 19341 jcarrico@agi.com, tcarrico@agi.com
[3]Applied Technology and Engineering. P.O. Box 476, Bertram, TX 87605 cfd@.thegateway.net

Abstract

The authors present several lunar landing trajectory strategies, including those used on the Apollo, Ranger and Surveyor programs; some planned for a commercial lunar mission; and some new techniques based on artificial intelligence. The paper describes the complete strategies for trajectory design from Earth-launch to Lunar landing. This includes a comparison between using Earth and Lunar orbit strategies versus direct ascent and direct descent methods. Closed-loop landing controls for the descent to the Lunar surface are also discussed. Each of these cases is modeled with a high-precision numerical integrator using full force models. The authors document and compare the maneuvers, fuel use, and other parameters affecting the transfer and landing trajectories. In addition, the authors discuss methods to expand the launch window. The fully integrated end-to-end trajectory ephemerides are available from the authors in electronic ASCII text by request.

Background

The work presented in this paper originally started in support of developing a software framework in response to the NASA Space Exploration Initiative[1]. In developing the software framework, it became apparent that there was not a lot of recent literature on the methods of Lunar landing. This current work is the result of investigating how Lunar landings were achieved on previous missions, and modeling these techniques with modern software. The results of modeling previous techniques with high-precision numerical integration are presented. In addition, some work has been done to use new methods, and a subset of that work is also presented.

Earth-to-Moon Transfers

Earth-to-Moon transfer trajectories can be described in three major phases: Leaving the Earth, transferring from the Earth to the proximity of the Moon, and approaching the Moon.

Leaving the Earth

There are two main ways to launch from the Earth into a transfer trajectory: either by direct ascent into the trans-Lunar trajectory or by first inserting into an Earth parking-orbit and then, after a specified coast time, executing a Trans-Lunar injection (TLI) maneuver. This second method is sometimes called "Launch-Coast-Burn." Often the choice between the two methods is

simply based on the capabilities of the launch vehicle. A review of the early missions seems to indicate that the first missions were direct ascents, but soon the launch-coast-burn was used when the technology became available. The Soviet Luna missions 1-3 used direct ascent[2], but most if not all the Luna missions afterwards used launch-coast-burn. The Soviet Zond 4[3] used launch-coast-burn. , as did the Ranger 7-9 missions.

An early NASA technical report entitled "Surveyor Project Final Report[4]" states:

> *Surveyors I, II, and IV were injected into translunar trajectories via the direct-ascent mode; Surveyors III, V, VI, and VII used the parking-orbit ascent mode. The parking-orbit ascent mode was clearly superior from a mission design standpoint, since, using a parking-orbit ascent, it was geometrically possible to launch on any day of the month.*

Indeed, using the launch-coast-burn method allows transfers to the Moon on any day of the month. The maneuver magnitude ("burn") has complete responsibility for establishing the apogee at or near the Lunar orbit distance from the Earth. The Launch time has total control over and establishes the right ascension of the ascending node (RAAN), and the coast time establishes the direction of the line-of-apsides. Using the launch time to control the RAAN allows the orbit plane to be rotated so as to contain the Moon at Lunar encounter. The coast time is adjusted to put the apogee of the transfer orbit near the Moon's orbit. Combined, these controls allow the transfer trajectory to encounter the Moon at any day of the month. All the trajectories produced for this study use a launch-coast-burn ascent from Earth.

Transfer Trajectories

There are several types of transfers from the Earth to the Moon. Most missions flown up to this point have used a simple ballistic transfer that can be thought of as a very eccentric Earth-centered ellipse with its apogee at the Moon. (This description, of course, doesn't account for the gravity of the Moon, but remains useful.) If the apogee is just at the Moon's distance, the transfer time will be about 5 days. If the TLI is greater, then the apogee will be beyond the Moon, and will require a greater Lunar Orbit Insertion (LOI) maneuver to capture at the Moon. Four examples are shown in Figure 1: A 5 day transfer, a 4-day, a 3-Day, and a 34 hour (1.4 Day), the last being the time-of-flight used for the Luna-1 mission[2], the first mission to the Moon.
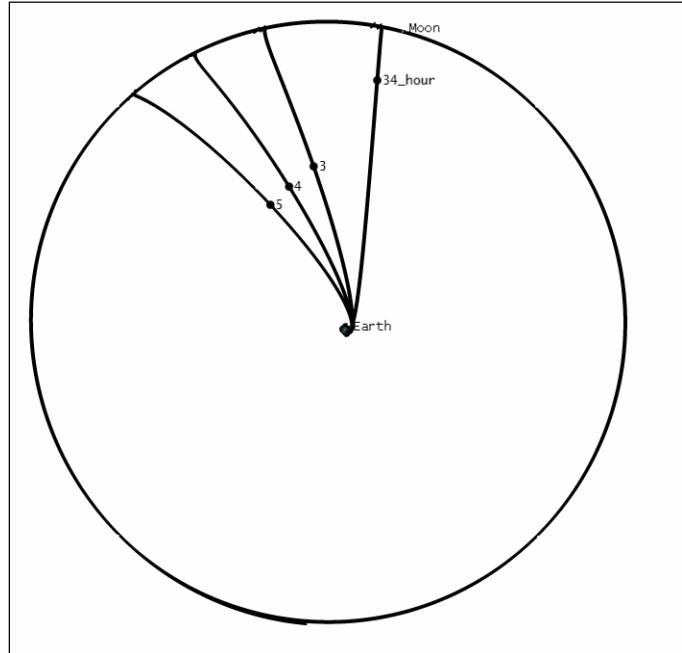

Figure 1: Ballistic Transfer is Earth-Centered Inertial Coordinates

It is often more insightful to plot the trajectories in a rotating system, with the Earth-Moon line fixed. These same examples are shown in Figure 2. The Soviet Luna 1 flew a 34 hour (1.4 day)

transfer[2]. Luna 9, the first spacecraft to perform a soft landing on the Moon, used a 3 day 7 hour transfer[2]. Apollo 11 used a 72 hour (3.0 day) transfer[5]. Lunar Prospector[6] flew a 105 hour (4.375 day) transfer.
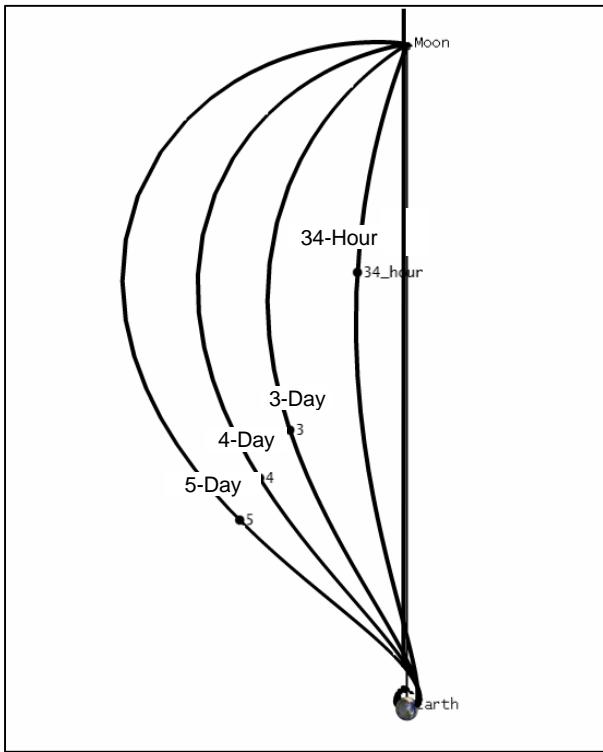

Figure 2: Ballistic Transfers in Earth-Moon Rotating Coordinates

In order to expand the launch window, several missions have added phasing loops before the final transfer from the Earth to the Moon. Clementine[7,8,9,10] used 2½ phasing loops, which could be adjusted in orbit period with perigee maneuvers to allow for more launch days per month while maintaining the same arrival day (to meet lunar lighting conditions.) An example from the present work, with 3½ phasing loops, is shown in Figure 3. This figure is shown in the Sun-Earth rotating coordinate system which separates the phasing loops, making it easier to understand and analyze. The use of rotating coordinates is common practice, and each system has its own purpose.
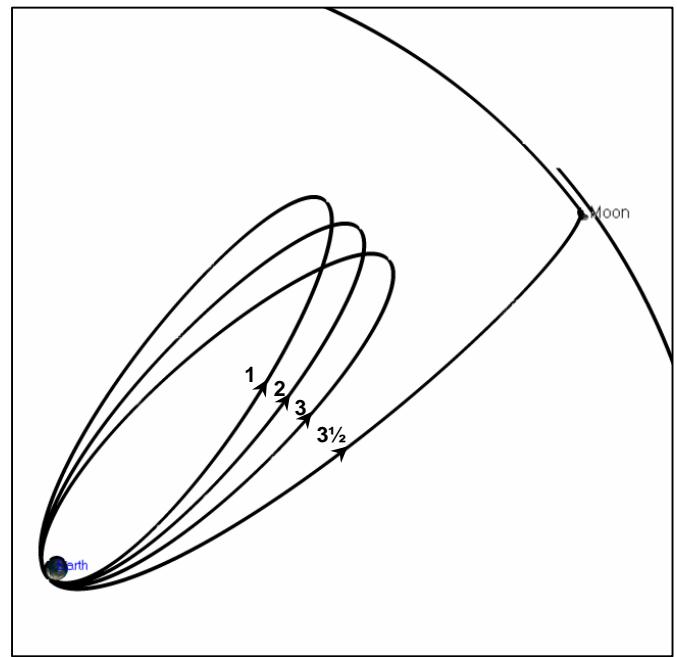
Another method of Lunar transfer is the Weak Stability Boundary (WSB) transfer[11,12,13,14,15,16]. The transfer trajectory leaves the Earth with an apogee around 1.5×10^6 km, and falls back into Earth orbit, but with a radius of perigee increased by the Sun's perturbations so that it co-orbits the Earth with the Moon. As a result, the spacecraft can enter lunar orbit with no maneuver, although it is a highly unstable orbit, and must be controlled. This is shown in Figure 4 in Earth Inertial coordinates and Figure 5 in Sun-Earth rotating coordinates.

Figure 3: 3½ Phasing Loop Transfer in Sun-Earth Rotating Coordinates

Although the TLI maneuver for the WSB is greater than for the standard ballistic transfer, there can be a lunar capture ΔV savings of about 25% when capturing into a Lunar orbit. The Hiten mission[17] (originally called Muses-A) performed such a capture in October, 1991.
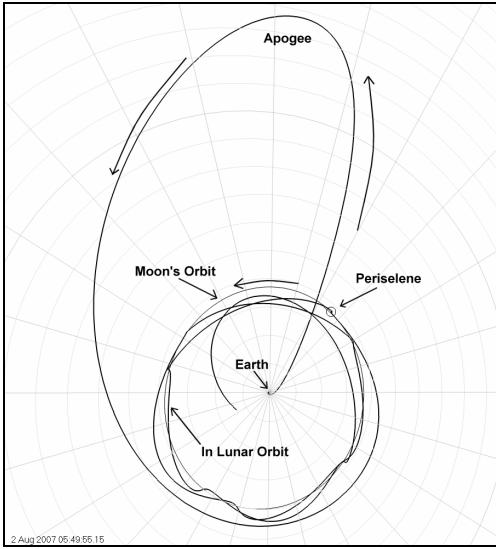
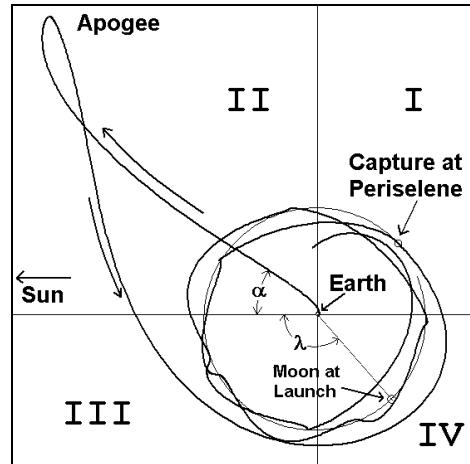**Figure 4: WSB in Earth Inertial Coordinates**

Figure 5: WSB in Sun-Earth Rotating Coordinates

There have also been proposals and studies of first transferring to a Lissajous orbit at the Earth-Moon L1 point, possibly rendezvousing with a space station there, and then continuing on to Lunar orbit[18,19,20,21,22]. This is sometimes referred to as an "L1 Gateway" trajectory. Transfer trajectories have also been proposed that first transfer to the Earth-Moon L2 libration point, possibly rendezvousing with a space station there[23], before descent to the Moon.

Smart-1 is a unique mission in that it used a low-thrust ion engine to transfer from a geostationary transfer orbit to Lunar orbit. From a NASA Lunar mission webpage[2]:

> *The SMART-1 spacecraft launched on 27 September 2003 from Kourou, French Guiana as an auxiliary passenger on an Ariane-5 Cyclade which launched two other large satellites as its primary payload. It was put into a geostationary transfer orbit, 742 x 36,016 km, inclined at 7 degrees to the equator. The spacecraft used its ion drive over a period of 14 months to elongate its Earth orbit and utilized three lunar resonance maneuvers in August, September, and October 2004 to minimize propellant use. Its final continuous thrust maneuver took place over 100 hours from 10 to 14 October 2004. Lunar orbit capture occurred on 13 November 2004 at a distance of 60,000 km from the lunar surface. The ion engine began firing in orbit at 05:24 UT (12:24 a.m. EST) on 15 November to start a 4.5 day period of thrust to lower the orbit. The first perilune took place on 15 November at 17:48 UTC (12:48 p.m. EST) at an altitude of about 5000 km above the lunar surface. The engine was then used to lower the initial 4962 x 51477 km altitude, 5 day, 9 hour period, 81 degree inclination orbit, putting SMART-1 into a 300 x 3000 km polar orbit.*

Approaching the Moon

This study compares two methods of approaching the Moon. The first is a direct Lunar descent, in which the transfer trajectory from the Earth is targeted to a direct Lunar landing. The second method involves capturing into a Lunar parking-orbit from the translunar trajectory by executing a retrograde Lunar Orbit Insertion (LOI) maneuver at or near periselene. After orbiting in the capture orbit for one or more orbits, a Descent Orbit Insertion (DOI) maneuver is performed to

lower periselene and start the descent to the Lunar surface. For this study, a circular Lunar parking-orbit based on the Apollo missions of 60 nm (111 km) altitude is used.

Mission Examples

When researching the present work, the study of previous missions was invaluable. In particular, the Surveyor missions were helpful for the direct Lunar descent trajectories, and the Apollo missions were the model for the Lunar parking-orbit. The final Apollo descent was also the model for the approach and landing maneuvers, and is described in greater detail later.

Surveyor 1 was launched directly into a lunar impact trajectory. A staged solid retro-rocket was used to slow the spacecraft as it approached the Lunar surface, that is, without inserting into a lunar parking-orbit. It then used vernier engines to affect a soft landing. Surveyor 3 used a launch-coast-burn ascent to achieve a Lunar transfer trajectory. The descent to the Lunar surface was achieved using the same technique as Surveyor 1. This site was later visited by Apollo 12. Surveyor 5 also used the launch-coast-burn ascent, and then during operations the trajectory was modified to compensate for an onboard failure. Surveyor 6 had the same trajectory profile as Surveyor 3, but performed a pre-planned hop on the Lunar surface.

A Proposed Commercial Mission: *Blastoff!*

Some of the work presented in this study was originally investigated for a proposed mission that never flew. *Blastoff!* was a commercial entity funded by *Idealabs!* in 2000. The company planned a commercial mission to the Moon that would have placed rovers near the Apollo landing sites. Nominal *Blastoff!* trajectories used the Lunar Surveyor direct descent approach, with 2 stacked solid motors: a Star 37 and a Star 20. The Star 37 was to be used to perform the TLI out of Earth orbit, and the Star 20 would have been used to slow the Moon-centered-fixed velocity above the Lunar surface prior to landing engine ignition. The Lander was then to use a mono-propellant hydrazine propulsion system to control the vertical drop rates. This trajectory is numerically simulated with a closed-loop feedback control that counters the Moon's gravity to achieve a constant descent rate.

The direct descent design of the *Blastoff!* mission was driven by the need to minimize financial cost and achieve Lunar landing as soon as possible after launch. It was quicker and cheaper to acquire solid engines than to build a bipropellant system from scratch and this design enabled the company owners to meet their schedule. The spacecraft would have been launched on an Athena II Launch vehicle, and the monopropellant landing system would have also been used for midcourse control during the cruise phase.

Blastoff! considered a classic 3.5 phasing loop approach where the first loop was slightly stunted, as performed by Clementine. A single phasing loop was also considered. In addition, another approach considered was to use 1 phasing loop with a 3 phasing loop backup: If the launch dispersions were too great to perform the mission, a 3 phasing loop strategy allowed the spacecraft to coast until the next month, in which case the transfer could be completed, although to an alternate landing site.

Trajectory Examples

Several trajectories for this study were calculated, and are described in detail in the following sections. The same numerical methods were used to calculate all trajectories.

Numerical Methods

The trajectories presented have been calculated using numerical integration with full-precision force models, including the effects of the gravity of the Earth, Moon, and Sun, as well as non-spherical gravity of the central body: a 21x21 Earth gravity field near the Earth, an 8x8 Earth gravity field in cislunar space, and an 8x8 Lunar field when near or around the Moon.

During the low-Earth parking-orbit, the translunar trajectory, and the Lunar parking-orbits, an error controlled dual-order variable-step Runge-Kutta algorithm was used to propagate the trajectories using Cowell's formulation of the equations of motion. During the closed-loop control of the final descent phase the same numerical integrator was used, but the maximum step size was set to 1.0 second for some runs, and to 0.1 second for others (as discussed below).

The software used for these studies is the *Satellite Tool Kit/Astrogator* module[24] written by Analytical Graphics, Inc.[25] in cooperation with the NASA Goddard Space Flight Center (GSFC) Flight Dynamics Analysis Branch (FDAB). *STK/Astrogator* was first used to analyze and plan maneuvers operationally for the WMAP mission[26]. *Astrogator* is the commercialized version of *Swingby*[27] developed at the NASA GSFC Flight Dynamics Division (now the FDAB), which was used to analyze and plan maneuvers operationally for Clementine (DSPSE)[28], Lunar Prospector[6], WIND[29,30,31], SOHO[32], and ACE[33]. The first commercialized version before *Astrogator* was called *Navigator* which was used to fly the AsiaSat-3 rescue mission around the Moon[34].

For trajectory design and maneuver planning, *Astrogator* uses an iterative differential correction method to solve a series of targeting problems. These targeting problems are set up (or "profiled") and called automatically, allowing sequential problems to be solved, such as coarse, fine, and very fine targeting problems. The user sets up the profiles, selecting the controls and desired constraints for each, and specifies other parameters such as step-sizes and convergence tolerances. *Astrogator* can also be used with optimization methods, such as *STK/Analyzer*, although this was not needed for the current analysis.

For the closed-loop control analysis described in the Lunar Descent section, *Astrogator's* extensible functionality was used. Specifically, some custom plug-in engine models were written in VBScript, which *Astrogator* can call at run-time without the need to modify *Astrogator* itself. This plug-in capability is documented in the *Astrogator* on-line help system.

Transfer Trajectory Simulations

For comparison purposes, all the following trajectories were targeted to achieve a landing at the same landing site (latitude 10 deg, longitude 340 deg) on 24 February 2010 06:00 UTC. The ΔV values reported for each transfer trajectory include the impulsive and finite maneuvers needed to descend to the lunar surface. The details of the powered descent modeling is describe later in the paper, and only one method is used in this section for reporting, the kinetic landing algorithm.

5-day Transfer to Lunar Parking-Orbit

The first trajectory is a standard 5-day transfer from the Earth to the Moon, and is the 5-day transfer shown in Figure 1 and Figure 2. Other than a longer time-of-flight, it is very similar to the Apollo trajectories. A multi-profile targeting sequence was used to design this trajectory. Using a first guess for the initial TLI maneuver based on previous studies (3.14 km/s), the Launch and Coast were varied so that when the spacecraft was at approximately Lunar orbit distance (400,000 km form Earth) the difference between the spacecraft's Right Ascension and Declination compared to the Moon's same parameters are both zero. We call this "Δ-RA Δ-Dec" targeting. When this targeting profile has converged, then the Launch time, Coast time, and TLI ΔV are simultaneously adjusted to achieve a guess at the B-Plane[35] parameters B•T and B•R (-5000 km, 5000 km), as well as time of flight. After this, the launch-coast-burn parameters are adjusted to achieve a periselene altitude of 60 nm (111 km), an inclination of 165 degrees (similar to Apollo), and a 5 day time-of-flight. (5 days is approximately the value that yields minimum TLI and LOI ΔV.) After this, the LOI maneuver is targeted to achieve a circular Lunar parking-orbit, which at 60 nm has a period of about 2 hours. About two revolutions after the LOI, the trajectory passes over the landing site, and the descent phase was computed, as described later. The descent phase includes a DOI maneuver of about 29 m/s, and the integrated ΔV of the powered descent to the surface. Table 1 summarizes the major features of this trajectory.

Launch	19 Feb 2010 00:23 UTC
Coast	35 min
TLI	3.137 km/s
LOI	816 m/s
DOI	29 m/s
Powered Descent ΔV	1915 m/s

Table 1: 5-Day Transfer to Lunar Orbit Mission Summary

5-day Transfer to Direct Lunar Descent

A 5-day transfer to a direct Lunar descent is shown in Figure 6. The trajectory is shown in the Moon-Fixed coordinate system. Targeting this trajectory starts off very similar to the previous. The initial Δ-RA Δ-Dec targeting is followed by B-Plane targeting with a time of flight (TOF) constraint. However, in this case, B-Plane values are used that would cause the trajectory to impact the Moon (3000 km, 128 km). The trajectory never hits the Moon, however, as the propagation is stopped at a radius of 50,000 km from the Moon's center.
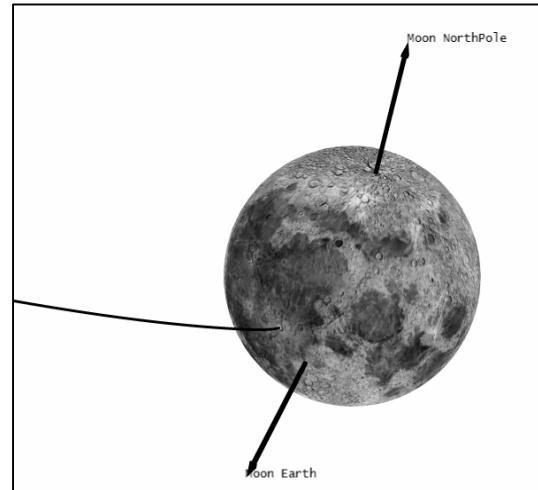

Figure 6: Direct Lunar Descent

After the B-plane targeting has converged with a TOF constraint a staged braking maneuver is inserted, and is targeted to burn until only a specified Moon-centered-fixed excess velocity of

1500 m/s remains. The closed-loop descent control law is also added (as described later.) Then the launch-coast-burn values are varied to achieve the desired latitude, longitude, and epoch of landing. Each iteration of the targeter includes a complete numerical simulation of the Lunar descent. *Astrogator's* homotopy search method was useful in solving this non-linear problem in some cases.

After each time the trajectory converges, the altitude of the braking maneuver and residual excess velocity are adjusted until the Lander has minimal fuel when landed. Table 2 summarizes the major features of this trajectory, including the integrated powered decent ΔV.

Launch	19 Feb 2010 05:14 UTC
Coast	19 min
TLI	3.128 km/s
Staged braking maneuver	846 m/s
Powered Descent ΔV	2362 m/s
Altitude of braking maneuver start	324 km

Table 2: 5-Day to Direct Lunar Descent Mission Summary

3.5 Phasing Loop to Direct Lunar Descent

The 5-day transfer described above was augmented with 3 phasing loops, and re-targeted, and shown in Figure 3. The method was very similar to the 5-day transfer, except that a maneuver at the 3rd perigee (P3), just before the final transfer to the Moon, was needed to raise the apogee to reach the Moon. Table 3 summarizes the major features of this trajectory.

Launch	2 Feb 2010 01:44 UTC
Coast	35 min
TLI	3.096 km/s
P3 maneuver	41 m/s
Staged braking maneuver	832 m/s
Powered Descent ΔV	2350 m/s
Altitude of braking maneuver	324 km

Table 3: 3.5 Phasing Loop to Direct Lunar Descent Mission Summary

Weak Stability Boundary Transfer

For this study previous WSB trajectories[14,15] were analyzed and the geometry used as a first guess for targeting. The launch-coast-burn parameters were varied to achieve a line-of-apsides with a right ascension of 250 deg and a declination of -26 degrees, measured in the Sun-Earth rotating coordinate system. The TLI was varied to achieve C_3 energy of -0.723 km^2/s^2 in order to produce a radius of apogee at about 1.37×10^6 km. After this was achieved, the launch-coast-burn parameters were varied to achieve a desired epoch and X value, measured at the X-Z plane crossing in the Sun-Earth rotating frame.

In the Sun-Earth rotating frame, X is defined as the axis aligned from the Sun to the Earth, and Z is constrained towards the ecliptic's normal vector. The trajectory is shown in this frame in Figure 7. The line to the left of the Earth is the Sun-Earth line, which remains fixed in this coordinate system.

After this initial targeting, the same launch-coast-burn parameters were refined to achieve a desired velocity component in the X direction, this time measured in the Earth-Moon rotating frame instead. As shown in the literature[15], these two X axes line up at this transition.

After the trajectory has been targeted this far, a maneuver is inserted back at apogee, and the three components of the ΔV are used as controls to target the constraints set to the Moon-centered fixed Cartesian position of the landing site, in X, Y, and Z (all km). These are evaluated after stopping propagation on a Lunar altitude of zero. The next step is to refine the apogee maneuver to target on the latitude and longitude of the landing site, stopping at 200 km altitude, with the desired epoch as an additional constraint.
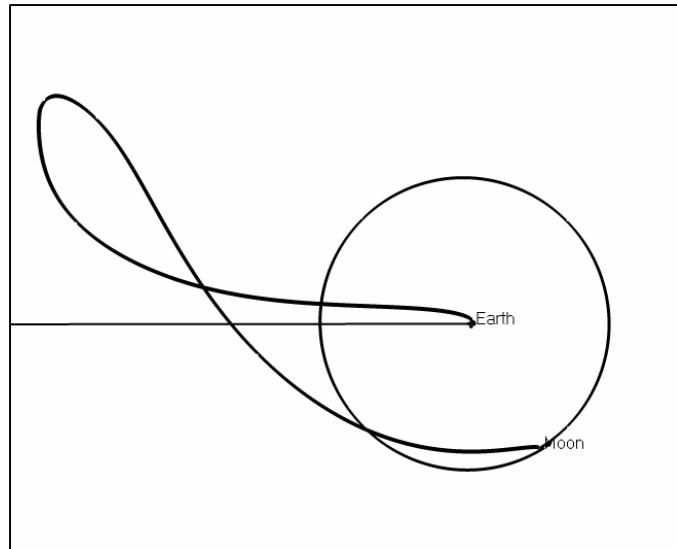

Figure 7: WSB Transfer in Sun-Earth Rotating Coordinates

When this has converged, a braking maneuver is inserted at 400 km altitude, and is targeted to leave an excess Moon-centered fixed velocity of 1500 m/s, to be consistent with the previously described direct descents. After the braking maneuver, the closed-loop descent control law is added. At this point the altitude of the braking maneuver and residual excess velocity could be adjusted to minimize the amount of fuel when landed, however, these first guesses based on the previous trajectories worked well. Table 4 summarizes the major features of this trajectory.

Launch	26 Nov 2009 04:41 UTC
Coast	78 min
TLI	3.194 km/s
Apogee maneuver	42 m/s
Staged braking maneuver	670 m/s
Powered Descent ΔV	2331 m/s

Table 4: Weak Stability Boundary Transfer Mission Summary

This WSB trajectory has been targeted without any optimization, and was constrained to a specific landing date. Based on previous work, it may be possible to lower the ΔV needed for this trajectory. The WSB LOI is a sensitive function of the landing date because landing date is directly correlated with the relative Sun-Earth-Moon geometry at encounter. WSB trajectories with unconstrained geometry at encounter can be optimized to minimize the orbital energy at periselene, which would minimize the LOI maneuver needed to enter a circular orbit.

Earth to Earth-Moon L1 to Lunar Orbit Transfer
This transfer involves first transferring the spacecraft from Earth to the Earth-Moon L1 point, staying in an L1 Lissajous orbit for two revolutions, transferring into Lunar parking-orbit, and

finally the descent. For this study an L1 Lissajous orbit with Z amplitude of about 20,000 km was chosen. The trajectory is shown in Figure 8.

To target the Earth-Moon L1 orbit the launch-coast-burn parameters were varied to achieve a Cartesian position of (0 km,0 km,10,000 km), measured in L1-centered Earth-Moon rotating libration-point coordinates. When this is converged, an L1 Orbit Insertion maneuver (L1OI) is inserted at the X-Z plane crossing, and targeted to achieve a subsequent perpendicular X-Z plane crossing. To target this, a constraint that the X component of velocity, V_X, must be zero is imposed. V_x is measured at the X-Z plane crossings in the L1-centered Earth-Moon rotating libration point coordinate system. After the first plane crossings converge to be perpendicular, the propagation is increased to the next X-Z plane crossing, and targeted to cross perpendicularly. When converged, the process is repeated, for several revolutions. As subsequent plane crossings are targeted, the previous crossings are not constrained to be perpendicular, and they vary slightly from this. At some point the magnitude of the corrections to the maneuver become un-physically small, and a station keeping maneuver can be used instead of the L1OI maneuver. The station-keeping maneuver is inserted several revolutions before the last targeted crossing, which minimizes the maneuver.
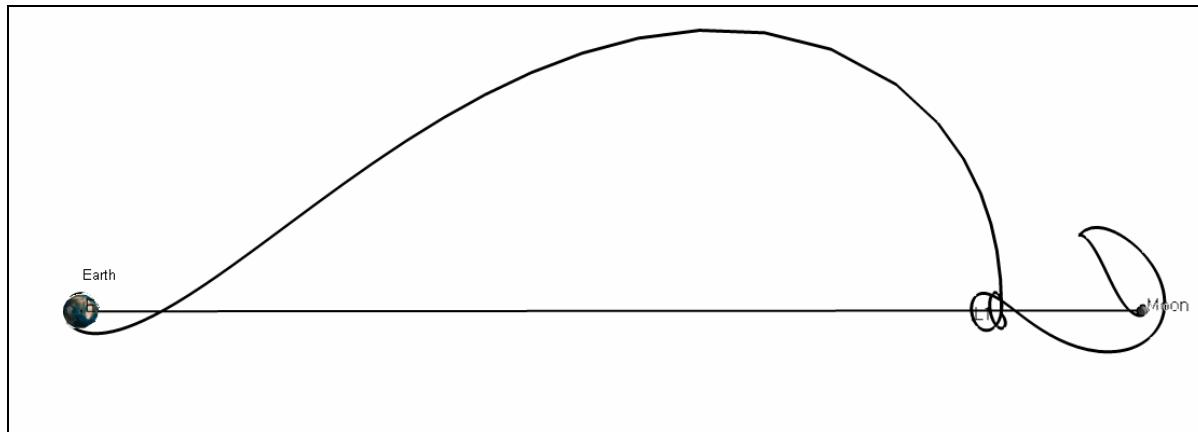

Figure 8: Earth to L1 to Lunar Landing in Earth-Moon Rotating Coordinates

The next step is to target the departure maneuver, after the number of desired revolutions in the Lissajous orbit. For this study, two revolutions in the Lissajous orbit were used from L1OI to the last plane crossing, lasting 22.5 days. A maneuver is used at an X-Z plane crossing a few revolutions before the desired departure time. As a coarse targeting step, the maneuver is first targeted like a station-keeping maneuver, which is to target subsequent perpendicular plane crossings. After this, the final crossing, two revolutions after the maneuver, is targeted with a slight velocity component towards the Moon. For this study, a V_X of 80 m/s worked well. This L1 departure ∆V was calculated to be 3 m/s.

After the departure maneuver, the trajectory heads towards the Moon. After Lunar closest approach (periselene at 7377 km altitude), a maneuver is performed at the next aposelene to lower periselene to 60 nm (111 km). The aposelene maneuver is also used to change the inclination of the Lunar orbit, so that, after a LOI circularization maneuver at periselene, the resulting Lunar parking-orbit passes over the desired landing site after 4 revolutions. (The Lunar

parking-orbit inclination in this case turned out to be 10 degrees.) Table 5 summarizes the major features of this trajectory.

Launch	22 Jan 2010 01:47 UTC
Coast	31 min
TLI	3.117 m/s
L1 orbit insertion maneuver	706 m/s
L1 departure maneuver	3 m/s
Perigee Lowering Maneuver	212 m/s
Apogee Lowering maneuver (Circularize)	623 m/s
DOI	22 m/s
Powered Descent ∆V	1952 m/s

Table 5: Earth to Earth-Moon L1 to Lunar Orbit Transfer Mission Summary

Transfer Trajectory Summary and Comparison

Table 6 displays the major features of the 5 transfer trajectories. The TOF for each is given, as measured from launch to landing. Note that the L1 transfer included an arbitrary 2 Lissajous orbits at the L1 point, so the TOF is given with the time spent at L1 included.

The total spacecraft (s/c) ∆V is the sum of all the maneuvers not including the TLI, since the TLI is usually performed by the upper stage of the launch vehicle. The ∆V without the powered descent is also given because there was no attempt to optimize the landings, and these could be lowered by further studies.

	5-Day to Lunar Orbit	5-Day to Direct Descent	3.5 Phasing Loop	WSB	L1
Launch (UTC)	19 Feb 2010 00:23	19 Feb 2010 05:14	2 Feb 2010 01:44	26 Nov 2009 04:41	22 Jan 2010 01:47
TOF (days)	5.23	5.03	22.18	90	33.2 (10.7)[†]
TLI	3.137	3.128	3.096	3.194	3.117
s/c ∆V w/o descent	845	846	873	712	1566
Total s/c ∆V	2760	3207	3223	3043	3518

Table 6: Transfer Trajectory Comparison

[†]The time of flight is only 10.7 days, when the 22.5 days spent in the Lissajous orbit at L1 is not included

The quickest transfers are the 5-Day transfers, as expected, and would presumably be more desirable for manned missions. A transfer to a station at the L1 point only takes about 10 days, not including the time at the station.

Targeting Specific Landing Sites

All trajectories were targeted to achieve the same landing site (latitude 10 deg, longitude 340 deg) on 24 February 2010 06:00 UTC. In order to affect a landing at this site without using too much fuel, the pre-landing trajectory, modeled as if the landing segment was not executed, should pass over the landing site. While this is a straightforward task for the direct descent trajectories, which can target the landing site directly, it is more complicated for trajectories that enter a Lunar parking-orbit prior to landing.

The Lunar orbit plane has a RAAN relative to the Earth-Moon line based on the TOF, as shown in Figure 9. Note that the 5-Day transfer has a relative RAAN of about 90 degrees to the Earth-Moon line, and as TOF is lowered, the trajectory approaches the Earth-Moon line.

The most straightforward method to cause the initial Lunar parking-orbit to pass over the landing site is to adjust the TOF. However, this can raise the TLI and LOI ΔVs, as well as possibly violate other mission requirements. Instead, it is sometimes possible to adjust the Lunar inclination. Another option is to stay in Lunar orbit until the natural precession of the orbit with respect to the Moon's surface causes the orbit to over-fly the landing site. If it does not fly over exactly, slight changes to the Lunar inclination, and possibly the orbit period can be made.
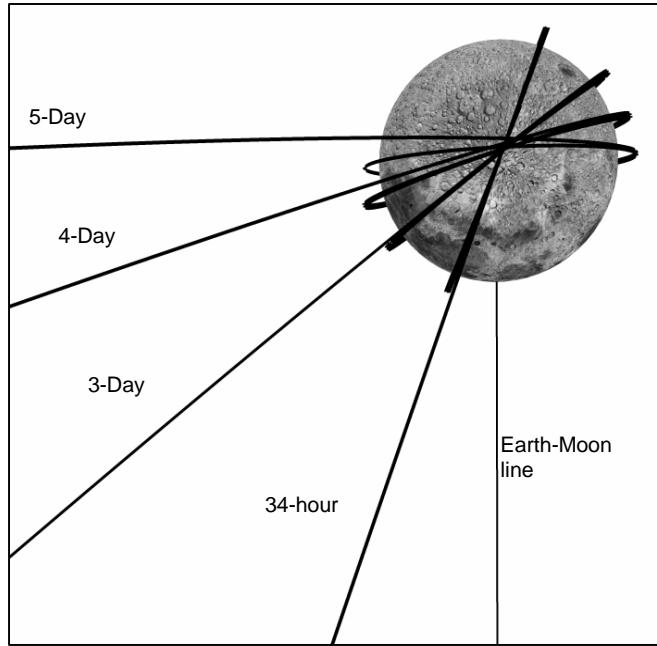

Figure 9: Different relative RAANs vs. Time-of-Flight in Earth-Moon Rotating Coordinates

For some of the trajectories above a simple adjustment of the inclination was enough, while others required several phasing orbits. For these, the number of orbits was increased until the ground track passed over the desired landing spot. (For this initial study the tolerance on the landing site was loose enough that this was not a hard task.) When such an orbit is identified, then the true anomaly of the DOI maneuver is adjusted to achieve the exact landing spot, usually by targeting on the exact desired latitude.

Lunar Powered Descent Trajectories

This section describes the powered descent methods, and is roughly based on the Apollo Lunar Module (LM) capabilities and landing strategy.   From the NASA technical memorandum "Apollo Lunar Descent and Ascent Trajectories[36]":

> *The LM powered descent trajectory design was established… as a three phase maneuver… to satisfy the operational requirements imposed of such a maneuver. The first phase, called the braking phase, is designed primarily for the efficient propellant usage while reducing orbit velocity and guiding to "high gate" conditions for initiation of the second phase, called the approach phase.   The term "high gate" is derived from aircraft pilot terminology for beginning the approach to an airport. The approach phase is designed for pilot visual (out the window) monitoring of the approach to the lunar surface. The final (or landing) phase, which begins at "low gate" conditions (again from pilot terminology) , is designed to provide continual visual assessment of the landing site and to provide compatibility for the pilot takeover from automatic control for the final touchdown on the surface.*

This study uses the Apollo[37] missions as reference and as a baseline from which future studies can be compared. The technique in this study[38] was to attempt to match certain Apollo velocities at their respective altitudes. The mass and propulsion properties for the Lander, dubbed Ke-V for this study[39], were also based on the Apollo LM Descent System, as shown in Table 7.

Fuel Mass	8165 kg (18,000 lbm)
Dry Mass	6531 kg (14398 lbm)
Specific Impulse, I_{sp}	311 s
Maximum Thrust	44042 N (9900 lbf)

Table 7: Lander Mass and Propulsion Values

Braking Phase

For the transfer trajectories that include a direct Lunar descent, a staged braking maneuver is used to achieved the typical Apollo high-gate 500 ft/s velocity at 7000 ft.

For the trajectories that include a Lunar parking-orbit before the descent, there are a series of braking maneuvers previous to 7000 ft that give a velocity of 500 ft/s at 7000 feet. This is shown schematically in the appendix. Screen captures from the numerical simulations in *STK* during the braking phase are shown in Figure 10 and a close-up in Figure 11 .
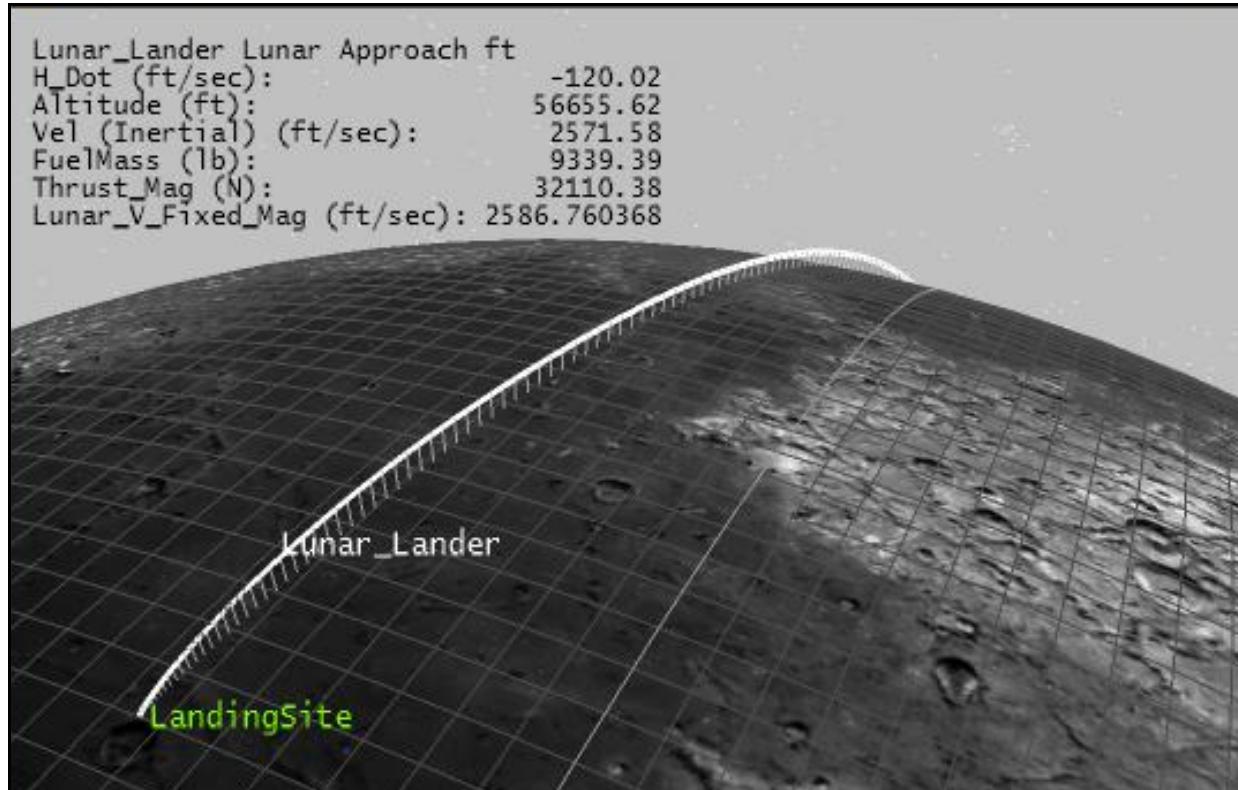

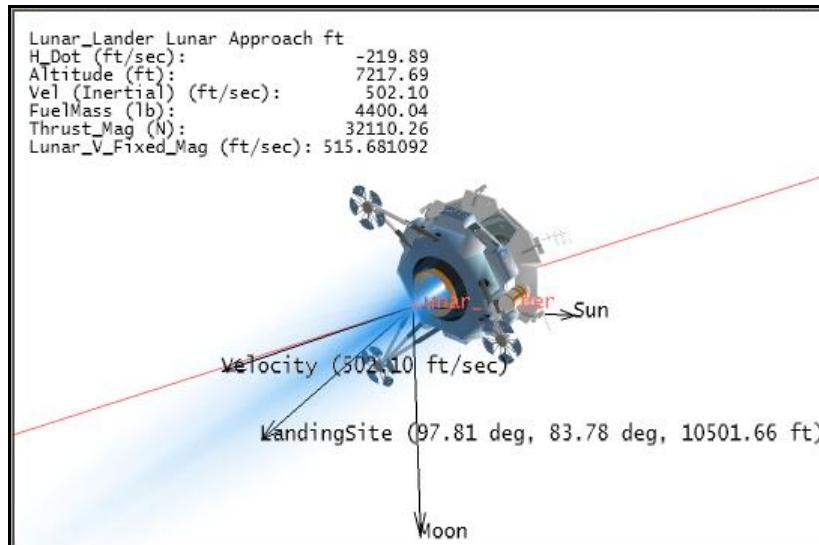**Figure 10: Screen Capture of Braking Phase from Numerical Simulation**

Figure 11: Screen capture of Ke-V during Descent Phase Numerical Simulation

After the standard Apollo lunar parking-orbit (60 x 60 nm altitude), the DOI maneuver lowers periselene to 50,000 ft (8.3 nm, or 15 km). At periselene, the Lander starts the retrograde braking maneuvers. The Apollo LM could not throttle continuously from full thrust to zero. The engine was not throttleable in the range from 60% to 90%. As a result, the controls laws for the LM accounted for this. In this study we model an engine with full throttle range.

The braking phase begins at periselene and the first maneuver lasts 26 seconds. The maneuver's thrust (the direction opposite the flames) is aligned about 5 degrees above the anti-velocity vector (measured in Moon centered fixed), and the throttle is at 10%. For Apollo, this maneuver gave time for the engine gimbal to align with the center-of-mass before maximum throttle was commanded. After this, a full throttle maneuver is executed for 150 seconds, with the thrust aligned 11 degrees above the anti-velocity vector.

Then the LM executed a series of different maneuvers and attitude changes for about the next 6 minutes until the high gate at 7000 ft. This study approximated this by varying a constant thrust efficiency to achieve a constraint of 500 ft/s at 7000 ft altitude, and used a constant attitude. The result of this study was a thrust efficiency of about 70% for this segment of the trajectory.

Approach and Landing Phases

The Approach phase begins at the high gate altitude of 7000 ft with a Moon-fixed velocity of 500 ft/s. This study compares two different closed-loop control laws used to model a soft landing on the Lunar surface, starting at the high gate. The two control laws are used to control the thrust of the descent engine. The first control law is based on using the landing thruster to affect a constant velocity descent rate. The second algorithm uses a Fuzzy Logic rule-based algorithm to control descent. Figure 12 is a screen capture from the Landing simulation.
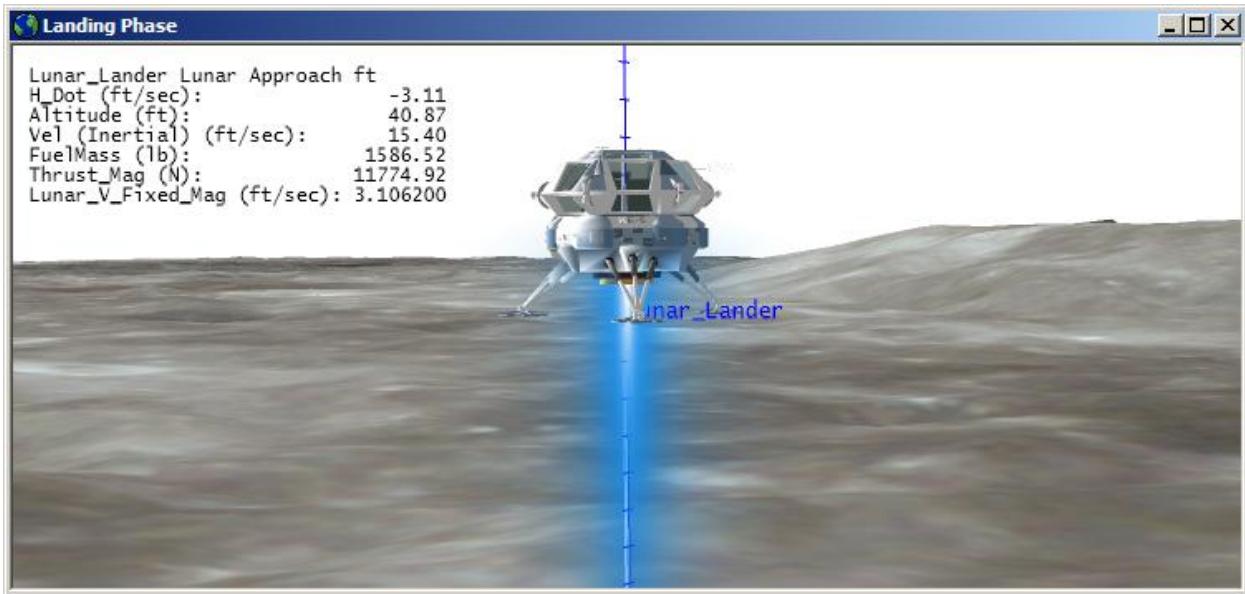
Figure 12: Screen Capture of Ke-V from Landing Numerical Simulation

Kinetic Controller

The first control law, dubbed the Kinetic Controller, varies the throttle value continuously to achieve a -4 ft/s Moon-fixed velocity at the low gate (150 ft). At 150 ft, a different algorithm is used to maintain a -3 ft/s altitude rate until landing.

The Kinetic Controller uses a simple algorithm to compute the necessary thrust. The controller is called between each propagation step, and the step size was limited to a constant. Every time the controller is called, it uses the current altitude, velocity, and mass to determine the appropriate thrust.

Some studies used a constant one second step (yielding 1 Hz), and this was compared with using a constant 0.1 second step (10 Hz). The fuel consumption differences were insignificant (about 0.02%).

To calculate the thrust, the time-independent equation of motion from classical physics is used:

$$a_d = (V_0^2 - V_f^2) / (2 (H_0 - H_f))$$

where H_0 and V_0 are the current displacement (altitude) and velocity, respectively. H_f is the altitude at low gate (150 ft), and V_f the desired rate at that point (-4 ft/s). The result then, a_d, is the desired acceleration. However, the commanded acceleration must also counter the gravitational acceleration of the Moon, g_M. Therefore the commanded thrust is calculated by adding the accelerations and multiplying by the total mass of the Lander:

$$Thrust = (a_d + g_M) \, Mass_{Total}$$

If the calculated thrust value is larger than the maximum thrust available for the landing engine, the maximum thrust is used. Once the Lander reaches low-gate, a different control law is used,

based on the altitude rate. It is a simple ratio of the current altitude rate, u_0 , to the desired rate, u_d, multiplied by the gravitational acceleration and the mass.

$$Thrust \ = \ (\ u_0 / u_d \ ) \ g_M \ Mass_{Total}$$

This control worked well to affect a soft landing in about 107 seconds from 7000 ft, and used about 1784 lb of fuel (811 kg). Figure 13 shows the altitude, velocity, and thrust over time as a result of running the simulation.
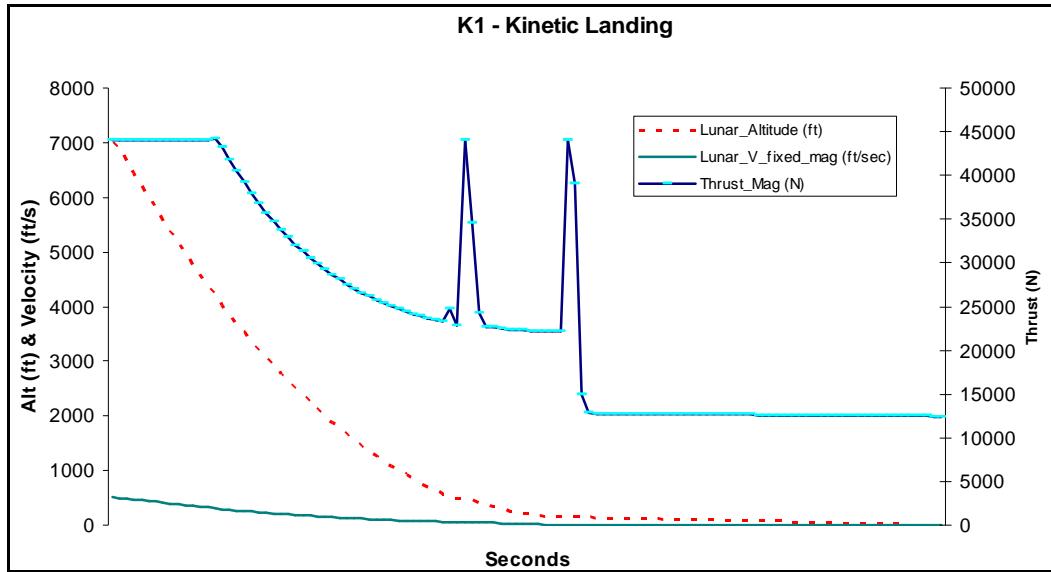

Figure 13: Altitude, Velocity, and Thrust Magnitude

Fuzzy Logic Controller

Fuzzy Logic was selected as the second mathematical model for calculating the requisite accelerations to land on the surface of the Moon. Fuzzy Logic is a proven method for the development of control laws in man-rated and other critical systems. It has also been implemented in various NASA systems and cited in numerous research and academic papers related to autonomous control in space.

Fuzzy Logic control is an evolution of the concepts defined by Lotfi Zadeh in his paper entitled "Fuzzy Sets, Information and Control.[40]"   Applied to control law development, it provides a method for the computation of linguistic control decision terms, such as Near, Far, Slow, and Fast and the transitions between. Used in a rule base, control laws can be developed such as:

> *"IF spacecraft is NEAR the Lunar Surface*
> *AND is going FAST*
> *THEN a LARGE ACCELERATION is required in the direction of the velocity vector."*

This method provides an understandable, maintainable method to encode subject matter expertise of astrodynamics specialists. With a significant cost associated with creating, constantly modifying and maintaining complex spacecraft control algorithms in a R & D environment, Fuzzy Logic provides an open dialog on descent trajectory analysis between astrodynamic specialists and software engineers, quite literally allowing for real time rule modification during

observation of the trajectories in 3D. This proved to be a powerful and time saving construct for analysis.

This paper discusses engine burns along the fixed Moon velocity vector for the Lunar landing sequence which alone is perfectly suitable for traditional control law methods. However, Fuzzy Logic provides a rapid means to modify and analyze various engine burn strategies and can be extended to simultaneously control spacecraft horizontal, vertical and attitude control to land in a desired location[1] allowing for analysis of highly complex, non-linear, multi-axis maneuvering, an area difficult to mathematically model.

The purpose of this research was to purport an analysis approach and environment for Lunar landing, not to seek adoption of any one technique or specific control law development. However, employing a set of standard tools, we were able to devise a method of Fuzzy Logic control that promises to offer a great deal of flexibility, simplicity and insight into Lunar landing behavior. The authors hope this contribution will lend itself to advanced engine, sensor design and mission planning.

Fuzzy Logic Determination of Requisite Acceleration for Lunar Landing

The *Satellite Tool Kit* was used as the Lunar landing simulation environment. With the *Astrogator* module, spacecraft can be modeled to a high level of fidelity and set into an accurate physics environment which includes gravitational forces, solar pressure and other space environmental conditions related to the Lunar mission. *Astrogator* is designed to model the physics of spacecraft flight and can fire engines based on various conditions or via external algorithms as in a closed-loop control law process. Controlling the engines in this simulation environment allows for accurate physics, numerous analytical tools and data outputs such as fuel consumption, burn rate and range rate.

The authors extended the engine model in *STK* to call an external Fuzzy Logic algorithm. The algorithm was developed in a commercial software product, *FuzzyTech*[41], and compiled into a callable library which received real numbers regarding velocity and range and returned acceleration. The desired acceleration was compared to the available thrust on the Lander and engines fired in *STK* to affect the maneuver. In this closed-loop process, the control algorithm is called every propagation step with relative speed and distance data. The algorithm calculates the acceleration required from the spacecraft's engine to achieve desired velocity and returns this value in ft/s^2. Acceleration was chosen over an earlier model returning thrust to provide an analysis environment independent of engine size.

The Fuzzy Logic model consists of a compiled algorithm designed in one commercial off the shelf (COTS) product, *FuzzyTech,* linked to another COTS product *STK*. To link these together, the authors coded a software component (COM Object) that is used to communicate between

---

[1] The authors assert, and intend to further study the notion of "best" ephemeris to landing by simultaneously controlling attitude, vertical and horizontal in response to a Fuzzy Logic analysis of the closing surface. Amplifying geographic information provided to the spacecraft as it descends regarding topography will allow small engine burns to adjust the trajectory early, alleviating larger, more costly burns closer to landing.

STK and the compiled algorithm, providing Fuzzy Logic I/O, performing various low level calculations, report writing and management of a waypoint to waypoint targeted velocity landing profile. The landing profile, loaded once at run time, is persisted in an Extensible Markup Language (XML) format, allowing the analyst to specify desired velocity/altitude pairs by simply editing a text document then propagating the descent trajectory. This is shown in Figure 14. XML will also lend itself to automation for trade studies on descent trajectory strategies.
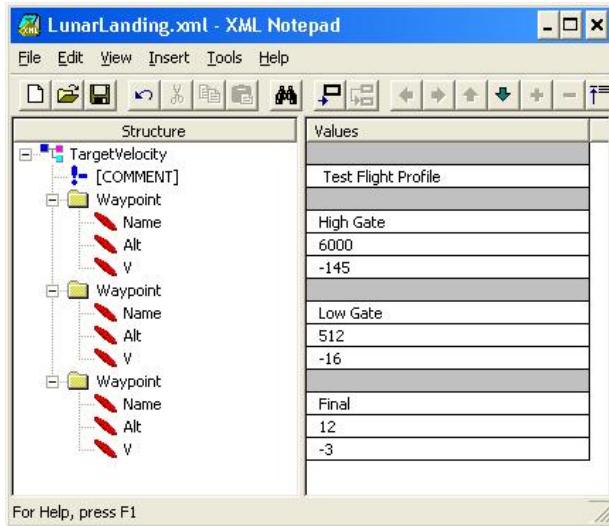

Figure 14: XML Lunar Landing Flight Profile

The Fuzzy Logic algorithm consists of two input sets, a rule set and an output set, which is shown in Figure 15. Each input in value is a real number that is converted into an element in one or more sets. However, unlike bivalent set logic, where a value belongs to a set or not (true/false), Fuzzy Logic membership in a set can be true, false, or somewhere in between.
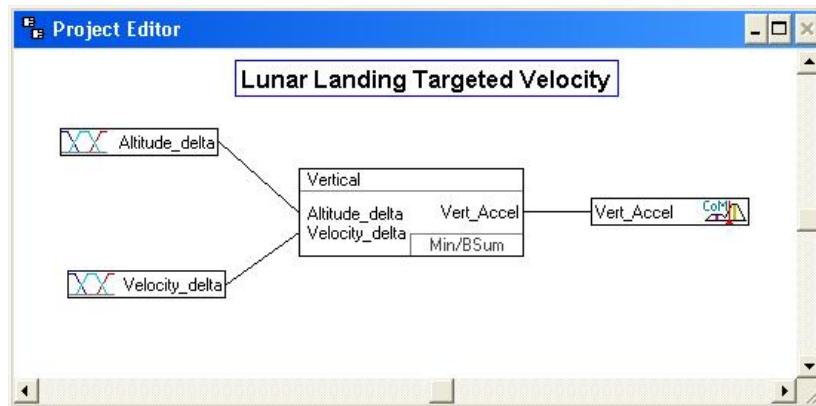

Figure 15: Lunar Landing Fuzzy Logic System

For this analysis each set's universe of discourse was defined in ranges representative of Apollo Lunar descent trajectories[36]. Review and modeling of the Apollo descent trajectories offered insight into the relationships between distances, velocities and thrust and baseline initial state values, providing a stepping off point for a Fuzzy Logic system design. For the purpose of this

analysis, this proved to be a suitable range providing a great deal of flexibility and acute control over the Lander as Fuzzy Logic took control at high gate. The ranges for sets, rules and acceleration output can be quickly modified to scale up or down to represent significantly different landing vehicles.

Input Fuzzy Set: Altitude Δ
Altitude Δ is the difference between the Lander's current altitude and the target altitude for the next altitude/velocity pair waypoint. For this analysis three overlapping sets were created to represent the concepts of far, near and at altitude. This is shown in Figure 16.
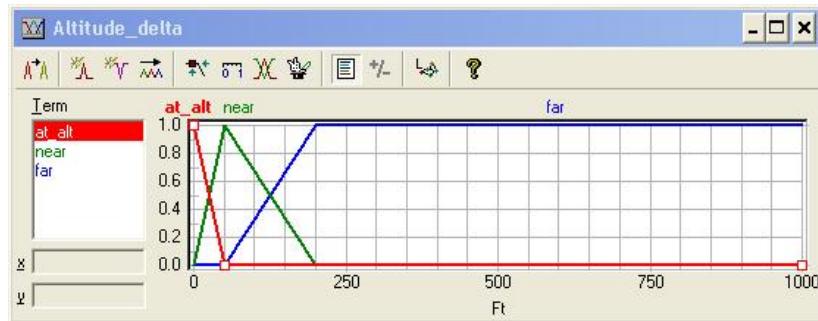

Figure 16: Fuzzy Input Set Altitude Δ

The shape of these sets provides the greatest range of values falling into the *far* set for all values greater than 50 ft. The geometric shape of *far,* with a wide range of values having membership value of 1.0 along the right side shoulder, provides for coarse control with few rules and little variation as it comes into a range where more acute control is desired. The shouldered sets also account for spacecraft conditions outside of the operating range of the controller.

Input Fuzzy Set: Velocity Δ
Velocity Δ is the difference between the Lander's current vertical velocity and the target velocity for the next altitude/velocity pair waypoint. The Fuzzy Logic algorithm uses Velocity (Moon Fixed) to calculate acceleration. At 7000 ft this value (in the simulation) is about 500 ft/s. The altitude rate at this point is – 200 ft/s.   As the trajectory approaches a more vertical orientation these numbers become near equal. By creating the simulation control on Velocity (Moon Fixed) the thrust removes the transverse rate of the Lander.

Similar to the altitude Δ Fuzzy set, velocity is represented by three overlapping sets, the shape providing a shouldered region for general control and velocities less than -75 ft/s (i.e., greater in magnitude), while more acute control over velocity occurs when greater than -75 ft/s (i.e., when at a slower landing speed). This is shown in Figure 17.
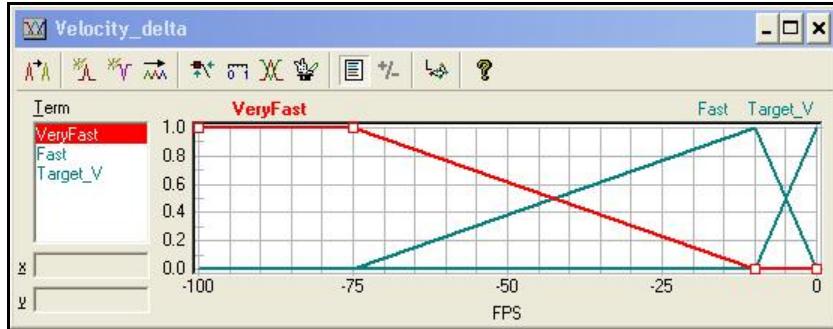
Figure 17: Fuzzy Input Set Velocity Δ

To illustrate how real numbers from *STK* are converted into Fuzzy Set values, the example below converts -60 ft/s into a Fuzzy Set value. The value from *STK* indicates a -60 ft/s Δ in the speed of the Lander compared to the current target velocity some distance away (Altitude Δ).

The number is passed into the algorithm and is converted into set membership values as shown in Table 8:

Real # Input from *STK*	Velocity Δ	Degree of Membership
	∈ Very Fast	0.77
-60 ft/s	∈ Fast	0.23
	∈ Target Velocity	0.00

Table 8: Velocity input set membership

This can be read as: The velocity Δ -60 ft/s is a member of the *VeryFast* variable to a degree of 77% and is a member of the *Fast* variable to a degree of 23% and is a member of the *Target_Velocity* variable to a degree of 0%.

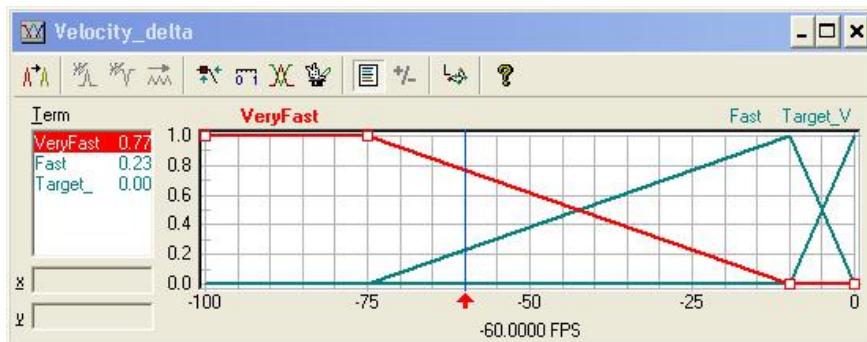Geometrically, the real number input value is represented in Figure 18:
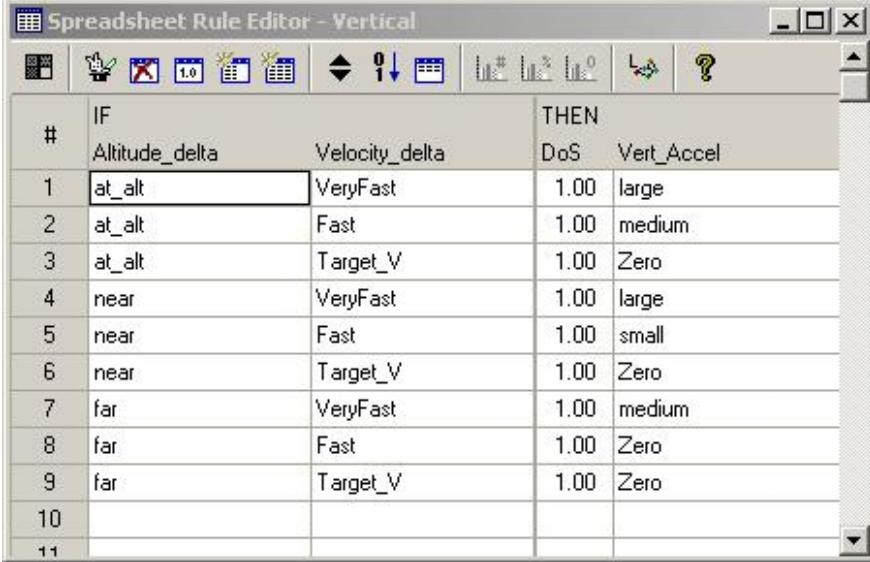

Figure 18: Fuzzy Input Set Velocity Δ for -60 ft/s from STK Simulation

Vertical Acceleration Rule Base
The inference rule set determines the acceleration set output and consists of antecedent and consequent (If, Then) statements. The rules are shown in Figure 19. (Note that deltas in velocity

and altitude were modeled to control the spacecraft, not with respect to the Lunar surface, but to specified points along the spacecraft's descent trajectory, allowing for comparative analysis.)

#	IF		THEN	
	Altitude_delta	Velocity_delta	DoS	Vert_Accel
1	at_alt	VeryFast	1.00	large
2	at_alt	Fast	1.00	medium
3	at_alt	Target_V	1.00	Zero
4	near	VeryFast	1.00	large
5	near	Fast	1.00	small
6	near	Target_V	1.00	Zero
7	far	VeryFast	1.00	medium
8	far	Fast	1.00	Zero
9	far	Target_V	1.00	Zero
10				
11				

Figure 19: Fuzzy Inference Rule Set for Acceleration

These rules fire in parallel in response to input from *STK*. For example, if **altitude Δ** is **far**, rules 7, 8 and 9 will fire. Since the output *Vert_Accel* is another Fuzzy Set, the inference rules provide membership values to the **Vert_Acel** set for calculation of a real number.

For this analysis, the membership in the output was calculated using a MIN function which sets the value of membership for a specific rule consequent by taking the minimum membership value of the altitude Δ and velocity Δ

> IF Altitude Δ is **far** (1.00) and Velocity Δ is **very_fast** (.85)
> THEN Vert_Accel is **medium** (.85)

Output Fuzzy Set: Vert_Accel
This output set models the acceleration required to arrive at the desired velocity for a given altitude as specified velocity/altitude waypoints in the XML file. This set is shown in Figure 20. As discussed in the previous paragraphs on rules, vertical acceleration is also a fuzzy set. However, *STK* requires a real number to calculate the engine thrust so a process called "Defuzzification" is required to convert the set membership into a real number for the simulation.
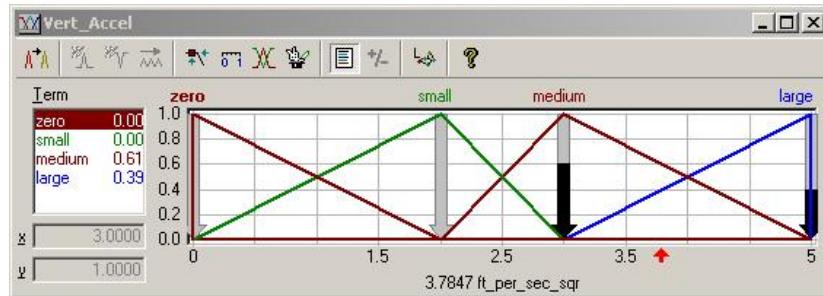
Figure 20: Fuzzy Output Set Vertical Acceleration

There are numerous methods available to calculate such a real number, for this paper the authors chose the Center of Maximum method (CoM). The CoM method of Defuzzification provides the best compromise for a real number output by calculating a weighted mean of the most typical (maximum) values for Acceleration by the inference results.

For example, the following conditions for spacecraft Δ altitude and Δ velocity return 3.78 ft/s^2 to *STK* which is converted into thrust (*Thrust = mass x acceleration*).

The most typical values for acceleration in this model are:

Zero = 0
Small = 2
Medium = 3
Large = 5

which result in a CoM Defuzzification of:

*(0.00 * 0 + 0.00 * 2 + 0.61 * 3 + 0.39 * 5) / (0.00 + 0.00 + 0.61 + 0.39) = 3.78*

Analysis of Fuzzy Logic

Two basic landing profiles where calculated using the Fuzzy Logic controlled velocity at velocity/altitude pairs, and are named "F1" and "F2" in this study. (The previous Kinetic lander is called "K1.") The calculated throttle value was updated at a rate of 1 Hz and 0.1 Hz to compare trajectory and fuel consumption. For the velocities in this research, the difference was negligible, as shown in Table 9.

Fuel Use (lbs)		
	1 Hz	0.1 Hz
F1	2494.72	2500.373
F2	2766.173	2787.226
K1	1784.027	1783.846

Table 9: Fuel Use as a Function of Simulation Step Size

Further analysis will be pursued on the update cycle rate to include broader control cycle ranges and velocities. This is important to tie the research to sensor and computer processing design.

Details on descent trajectory, acceleration and fuel are provided below.

Fuzzy Logic Landing Control Profiles
To understand the effect of the rules, 5 different simulations were run, as detailed in Table 10.

Flight Simulation	Description
F1	Altitude Velocity pairs taken from Apollo 17 Mission Report[42]
F2	Single Waypoint at landing
F2 Mod 1	Single Waypoint at landing – Rule Mod 1
F2 Mod 2	Single Waypoint at landing – Rule Mod 2
F2 Mod 3	Single Waypoint at landing – Rule Mod 1

Table 10: Fuzzy Rule Set Simulations

F2 used a single waypoint target of 12 ft and -3 ft/s. A single rule in the F2 simulation was further modified to compare flight profiles and fuel consumption, and were named "F2 Mod 1," "F2 Mod 2," and "F2 Mod 3." The rule that was modified was Rule 7: "IF *Far* AND *Very Fast* THEN *Large*." The consequent statement (THEN) was modified from *Large* to *Medium* and the Degree of Support (DoS) from 100% to 20%. DoS is an inference method which allows rules themselves to be weighted from 0 to 100 when the antecedent conditions are met.

Table 11 shows Rule 7 in simulation F2 and three modifications to the rule, simulations F2 Mod 1 to 3.

Flight Simulation	IF	AND	THEN	Degree of Support
F2	Altitude Δ =Far	Velocity Δ =Very Fast	Vertical Acceleration = Large	100%
F2 Mod 1			Vertical Acceleration = Medium	100%
F2 Mod 2			Vertical Acceleration = Medium	50%
F2 Mod 3			Vertical Acceleration = Medium	20%

Table 11: Rule 7 Modifications

This rule modification resulted in different landing profiles and fuel consumption. By modifying this single rule we adjusted the amount of acceleration to be used when at high altitude. Since the rules are independent from one another, and fire in parallel, other rules respond to the excess velocity as altitude decreases.

Removing velocity too early causes greater fuel consumption. Firing the engine *Large* at a *Far* distant to the surface, as in Simulation F2, removes the velocity early, resulting in a near constant velocity until an increase in thrust adjusts the velocity for targeted landing at -3 ft/s. This altitude, velocity, and mass flow rate history from this simulation are shown in Figure 21. (The mass flow rate is shown as negative in this figure representing the loss of mass as the Lander burns fuel.)
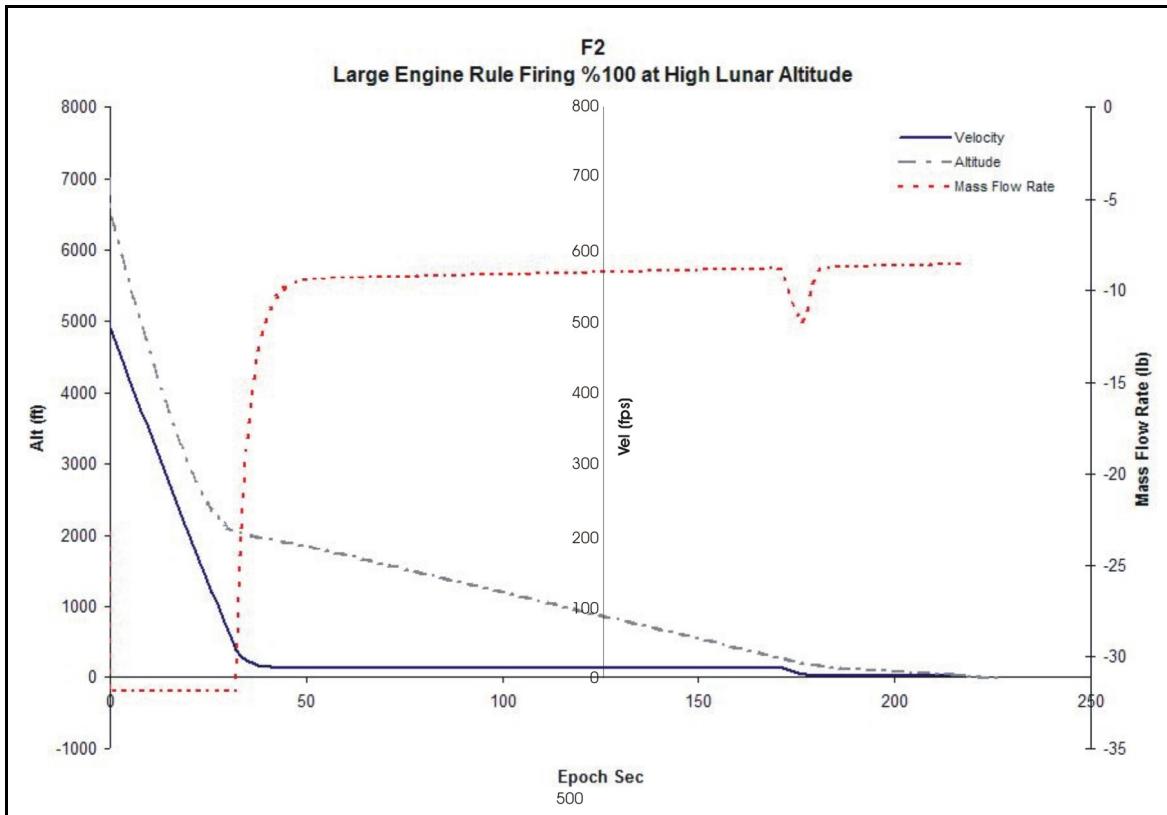

Figure 21: Simulation F2 (100% DoS at Higher Altitude)

By contrast, adjusting the rule to fire *Medium* to 20% at a *Far* altitude, as in Simulation F2 Mod 3, yields a more rapid overall descent with a much larger mass flow rate to adjust the velocity for landing. The results from this are shown in Figure 22.
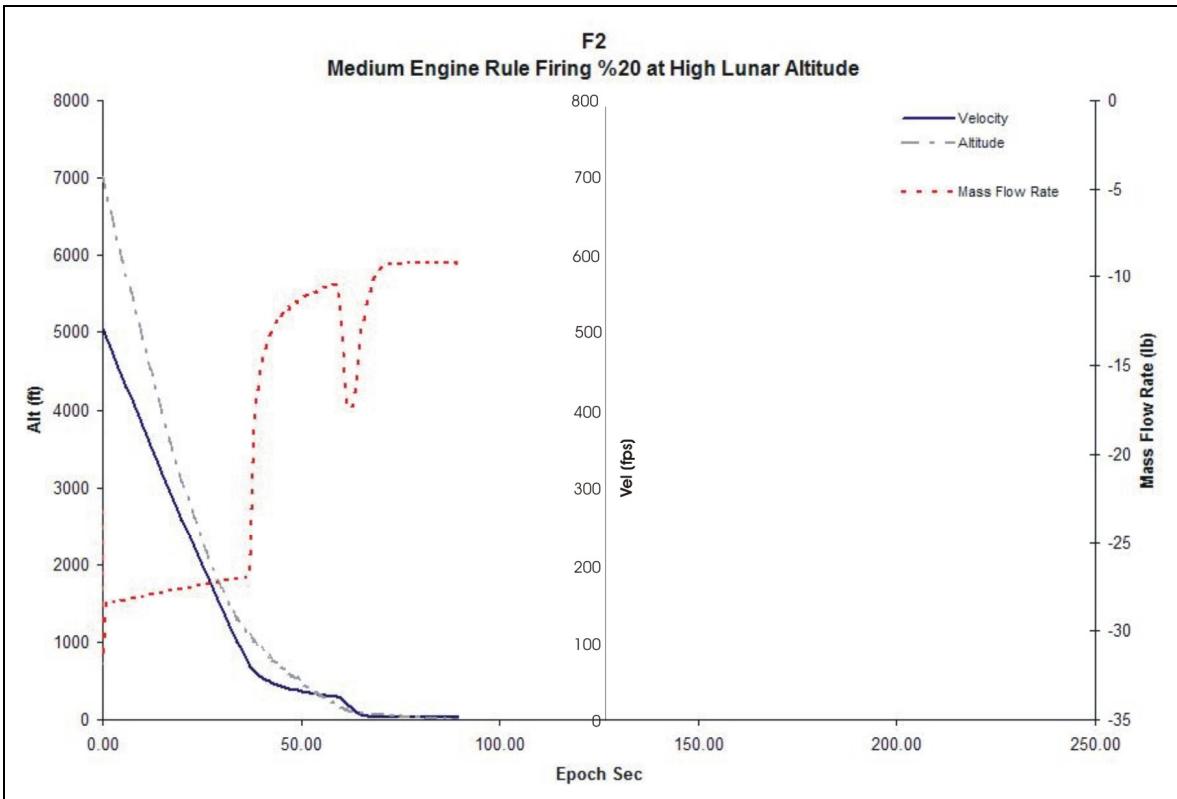
Figure 22: Simulation F2 Mod 3 (20% DoS at Higher Altitude)

Fuel consumption decreased the more the single rule was modified to decrease the application of thrust from a Far altitude. Switching the rule from **Medium** to **Small** resulted in too high a velocity for the closer rules to adequately remove. Table 12 shows the fuels use for each simulation, and these data are shown graphically in Figure 23

Flight Simulation	Fuel Consumption (lbs)
F1	2494.72
F2	2766.173
F2 Mod 1	1979.879
F2 Mod 2	1852.149
F2 Mod 3	1619.542
K1	1784.027

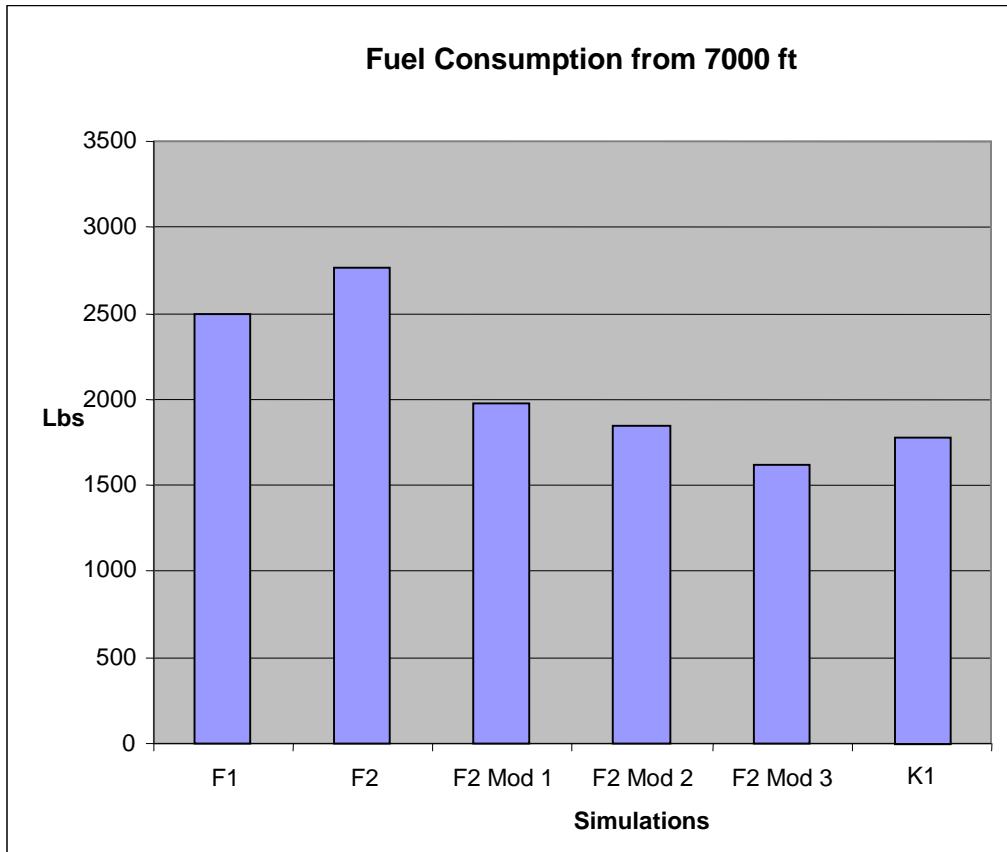**Table 12: Fuel Use for each Simulation**

Figure 23: Fuel consumption comparison for Fuzzy Logic F2 Flights from 7000 ft

F2 was a single waypoint descent profile. Observing the data from modification of a single rule provided insight into Δ velocity timing and has suggested further research into a more complex rule system that can take into account mass, human physical and mental comfort (g-force) to analyze these "bumps" in the graph where thrust is applied. The dramatic difference in fuel consumption (~1000 lbs) evidenced by moving these applications of thrust by modifying rules alone invites further refinement and analysis of the fuzzy input sets (altitude Δ and velocity Δ) where the shapes of the sets can further tune control.

Conclusions

The current study has resulted in fully numerically integrated trajectories from the Earth to a soft landing on the Moon. Several different types of transfer trajectories have been modeled, two types of Lunar approaches (Direct and Lunar parking-orbit), and two different control laws used for landing. These landings were based on Apollo strategies, and were successfully modeled using both a kinetic controller and a fuzzy logic controller. The Fuzzy-Logic controller used about the same fuel as the Kinetic, and was sensitive to various parameters.

This study has demonstrated that the current software trajectory and control technology is readily available and applicable to current analyses.

Future work

Now that the baseline trajectories have been calculated, the transfer trajectories can be optimized, and powered descent trajectories can be computed, and these compared with the baseline.

The effect of constraining the epoch of landing and methods to achieve specific landing sites using the WSB transfer require further investigation.

The affect of other mission constraints during landing, such as lighting conditions and obstacle avoidance must also be addressed.   These other mission requirements may affect the control law formulation and it is expected that the Fuzzy-Logic controller will be well-suited to account for these.   These preliminary results also indicate that changing the current fuzzy sets and other parameters may reduce the fuel use.

In addition, the Fuzzy Logic model may be extended to receive dynamic mass information which is expected to provide a more efficient method of timing the removal of velocity with respect to the next waypoint. Considerations will also being given to the difference of the determination of requisite acceleration magnitude and timing in terms of human comfort, pilot visibility and g-force limitations.
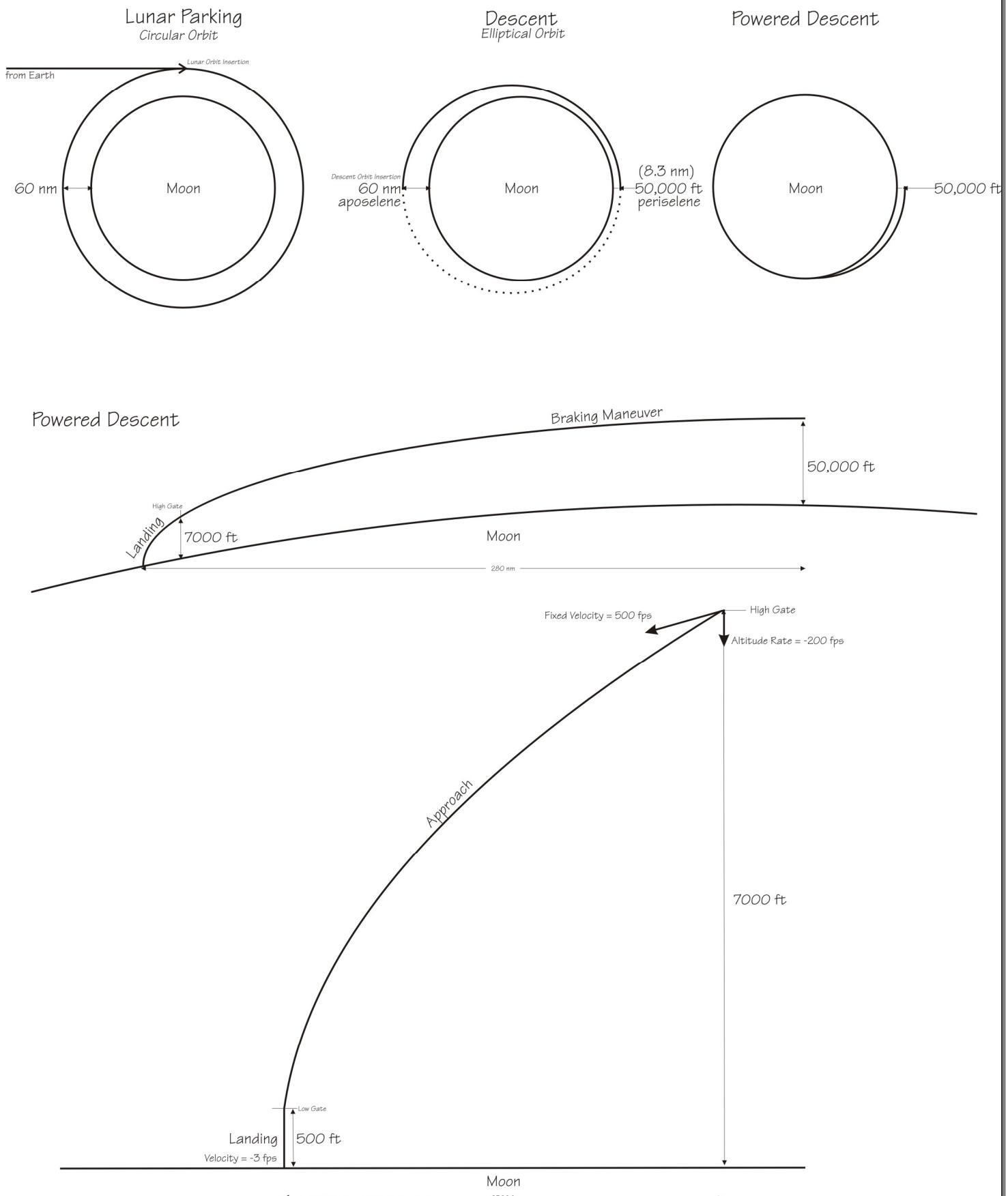
Because the overall goal of this work is to create an accurate physics-based environment and software framework to support Lunar trajectory design and control, future work will include support additional workflow and numerical simulation requirements.

Lunar Landing Numerical Simulations
Descent Trajectory from Lunar Circular Orbit

Appendix

Lunar Parking
Circular Orbit

from Earth

Lunar Orbit Insertion

Moon

60 nm

Descent
Elliptical Orbit

Descent Orbit Insertion
60 nm
aposelene

Moon

(8.3 nm)
50,000 ft
periselene

Powered Descent

Moon

50,000 ft

Powered Descent

Braking Maneuver

50,000 ft

High Gate

Landing

7000 ft

Moon

280 nm

Fixed Velocity = 500 fps

High Gate

Altitude Rate = -200 fps

Approach

7000 ft

Low Gate

Landing

500 ft

Velocity = -3 fps

Moon

8300 ft

Note: Not to scale, numbers representative

References

[1] NASA Space Exploration Initiative, announced at NASA Headquarters, Washington D.C., U.S. President Bush, 14 January, 2004

[2] NASA National Space Science Data Center (NSSDC) Lunar and Planetary Home Page (http://nssdc.gsfc.nasa.gov/planetary/) , specifically the link off this to the Moon home page (http://nssdc.gsfc.nasa.gov/planetary/planets/moonpage.html), September, 2005

[3] David Darling, The Encyclopedia of Astrobiology, Astronomy, and Spaceflight, (http://www.daviddarling.info/encyclopedia/ETEmain.html), September, 2005

[4] Jet Propulsion Laboratory "Surveyor Project Final Report," NASA Technical Report 32-1265, 1 July, 1969

[5] R. Godwin, (editor), "Apollo 11 - The NASA Mission Reports", Vol. I, p. 225, Apogee Books, 1999

[6] L. Lozier, K. Galal, , D. Folta, M. Beckman, "Lunar Prospector Mission Design and Trajectory Support,", AAS 98-323, 1998

[7] K.V. Richon, L.K Newman, "Flight Dynamics Support for the Clementine Deep Space Program Science Experiment (DSPSE) Mission," AAS 95-444

[8] D. Carrington, J. Carrico, J. Jen, C. Roberts, A. Seacord, P. Sharer, L. Newman, K. Richon, B. Kaufman, J. Middour, M. Soyka, "Trajectory Design for the Deep Space Program Science Experiment (DSPSE) Mission," AAS 93-260, Proceedings of the AAS/NASA International Symposium, Greenbelt, Maryland, April 1993

[9] J. Carrico, D. Carrington, M. Hametz, P. Jordan, D. Peters, C. Schiff, K. Richon, L. Newman, "Maneuver Planning and Results for Clementine (The Deep Space Program Science Experiment)," Paper No. AAS 95-129, AAS/AIAA Spaceflight Mechanics Meeting, Albuquerque, New Mexico, USA, February 1995

[10] D.W. Dunham, R.W. Farquhar, "Trajectory Design for a Lunar Mapping and Near-Earth-Asteroid Flyby Mission," AAS 93-145, Spaceflight Mechanics 1993, Vol. 82, Advances in the Astronautical Sciences, ed. R. Melton, pp. 605-624

[11] E.A. Belbruno, "Lunar Capture Orbits, A Method of Constructing Earth-Moon Trajectories and the Lunar GAS Mission," in: Proceedings of AIAA/DGLR/JSASS Inter. Propl. Conf., AIAA Paper No. 87-1054, (May 1987)

[12] E.A. Belbruno, "The Dynamical Mechanism of Ballistic Lunar Capture Transfers in the Four-Body Problem from the Perspective of Invariant Manifolds and Hill's Regions," Institut D'Estudis Catalans, CRM Research Report No. 270, (November 1994)

[13] E.A. Belbruno, R. Humble, J. Coil, "Ballistic Capture Lunar Transfer Determination for the U.S. Air Force Academy Blue Moon Mission," Advances in Astronautical Science, Spaceflight Mechanics, 95, AAS Publ., Paper No. AAS 97-171, (1997)

[14] E. Belbruno, J. Carrico, "Calculation of Weak Stability Boundary Ballistic Lunar Transfer Trajectories," Paper No. AIAA 2000-4142, AIAA/AAS Astrodynamics Specialist Conference in Denver, Colorado, USA, August 2000

[15] W.S. Koon, M.W. Lo, J.E. Marsden, S.D. Ross, "Shoot the Moon, Spaceflight Mechanics,", AAS Vol.105 Part II, 107-1181, 2000

[16] W.S. Koon, M.W. Lo, J.E. Marsden, S.D. Ross, "Low Energy Transfer to the Moon," Celestial Mechanics and Dynamical Astronomy, 81, 63-73. 2001

[17] H. Yamakawa, J. Kawaguchi, N. Ishii, H. Matsuo, "On Earth-Moon Transfer Trajectory with Gravitational Capture," in: Proceedings AAS/AIAA Astrodynamics Specialists Conf., Paper No. AAS 93-633, (August 1993)

[18] R. Farquhar, D. Dunham, "Libration-Point Staging Concepts for Earth-Mars Transportation," Manned Mars Missions: Working Group Papers, NASA M002, Vol. 1, NASA/LANL, June 1986, pp. 66-77; proceedings of a workshop at NASA Marshall Space Flight Center, Huntsville, Alabama, June 10-14, 1985

[19] R.W. Farquhar, D.W. Dunham, Y. Guo, J.V. McAdams, "Utilization of Libration Points for Human Exploration in the Sun-Earth-Moon System and Beyond," Proceedings of the 54th International Astronautical Congress of the International Astronautical Federation, Bremen, Germany, September-October 2003 (also: Acta Astronautica 55 (2004), pp. 687-700)

[20] W. Huntress, R. Farquhar, D. Stetson, B. Clark, J. Zimmerman, W. O'Neil, R. Bourke, "The Next Steps in Exploring Space" A Study by the International Academy of Astronautics, July 9, 2004

[21] G.L. Condon, C.L. Ranieri, C. Ocampo, "Earth-Moon Libration Point (L1) Gateway Station. Lunar Transfer Vehicle Kickstage Disposal Options," Libration Point Orbits And Applications, Parador d'Aiguablava, Girona, Spain , June 2002

[22] G.L. Condon, D.J. Pearson, "The Role of Humans in Libration Point Missions With Specific Application to an Earth-Moon Libration Point Gateway Station (AAS 01-307)", Advances in the Astronautical Sciences, Volume 109, Astrodynamics, p95, 2001

[23] R. Farquhar, "A Halo-Orbit Lunar Station," Astronautics & Aeronautics, June 1972, pp. 59-63

[24] J. Carrico, E. Fletcher, "Software Architecture and Use of Satellite Tool Kit's Astrogator Module for Libration Point Orbit Missions", Libration Point Orbits And Applications, Parador d'Aiguablava, Girona, Spain , June 2002

[25] Analytical Graphics, Inc., 220 Valley Creek Blvd., Exton, PA 19341, USA, Phone: 1.610.981.8000, info@agi.com, www.agi.com

[26] M. Mesarch, S. Andrews, "The Maneuver Planning Process for the Microwave Anisotropy Probe (MAP) Mission," AIAA 2002-4427, AIAA/AAS Astrodynamics Specialist Conference, Monterey, CA, USA

[27] J. Carrico, C. Schiff, L. Roszman, H.L. Hooper, D. Folta, K. Richon, "An Interactive Tool for Design and Support of Lunar, Gravity Assist, and Libration Point Trajectories," Paper No. AIAA 93-1126, AIAA/AHS/ASEE Aerospace Design Conference, Irvine, California, USA, February 1993

[28] J. Carrico, D. Conway, D. Ginn, D. Folta, K. Richon, "Operational Use of Swingby—an Interactive Trajectory Design and Maneuver Planning Tool—for Missions to the Moon and Beyond," Paper No. AAS 95-323, AAS/AIAA Astrodynamics Specialist Conference, Halifax, Nova Scotia, Canada, August 1995

[29] P. Sharer, , H. Franz, , Folta, D., "WIND Trajectory Design and Control," Paper No. MS95/032, CNES International Symposium on Space Dynamics, Toulouse, France, June 1995

[30] H. Franz, "WIND Nominal Mission Performance and Extended Mission Design," AIAA 98-4467, August 1998

[31] H. Franz, "WIND Lunar Backflip and Distant Prograde Orbit Implementation," AAS 01-173, AAS/AIAA Spaceflight Mechanics Meeting, Santa Barbara, California, USA, February 2001

[32] D.W. Dunham, S.J. Jen, C.E. Roberts, A.W. Seacord, "Transfer Trajectory Design for the SOHO Libration-Point Mission," IAF-92-0066, 43rd Congress of the International Astronautical Federation, Washington, D.C., USA, August/September, 1992

[33] P. Sharer, T. Harrington, "Trajectory Optimization for the ACE Halo Orbit Mission," AIAA-96-3601-CP (1996).

[34] J. Salvatore, C. Ocampo, "Mission Design and Orbit Operations for the First Lunar Flyby Rescue Mission," IAF-99-A.2.01, 50th International Astronautical Congress, Amsterdam, The Netherlands, October 1999

[35] W. Kizner, "A Method of Describing Miss Distances for Lunar and Interplanetary Trajectories," Ballistic Missile and Space Technology, III, 1961

[36] "Apollo Lunar Descent and Ascent Trajectories", NASA technical memorandum, NASA TM X-58040, March 1970, presented to the AIAA 8th Aerospace Sciences Meeting, NY, NY, 19-21 January, 1970

[37] Floyd V. Bennett, "Apollo Experience Report - Mission Planning for Lunar Module Ascent and Descent," NASA TN D-6846, June 1972

[38] M. Loucks, J. Carrico, T. Carrico, C. Deiterich, "A Comparison Of Lunar Landing Trajectory Strategies Using Numerical Simulations," International Lunar Conference, Toronto, CA, 2005

[39] Kevin Carrico, Impact Creative Services, www.impactcreative.net, 2005

[40] Lotfi A. Zadeh "Fuzzy Sets", Information and Control, 1965

[41] FuzzyTech, INFORM GmbH, Pascalstrasse 23, D-52076 Aachen, GERMANY, Phone: 2408-945680, hotline@inform-ac.com, http://www.fuzzytech.com/

[42] R. Godwin, (editor), "Apollo 17 - The NASA Mission Reports," Volume 1, Apogee Books, 2002